Laser Physics, Vol. 2, No. 6, 1992.

Original Text Copyright © 1992 by Astro, Ltd.
Copyright © 1992 by Interperiodica.

Thermal Nonlinear Effects in Optical Whispering Gallery Microresonators

V. S. Il'chenko and M. L. Gorodetskii

Physics Department, Moscow State University, Moscow 119899, Russia

Abstract – High-Q whispering gallery microresonators are proposed for use in quantum-nondemolition (QND) photon-number measurements via optical Kerr effect, and exhibit complex nonlinear behavior. This includes two types of thermal nonlinearity (multistability and low-frequency oscillations) at low levels of pump power $\simeq 10$ μW. Thermal nonlinearity of optical whispering gallery modes in fused silica microresonators has been investigated experimentally using a mode cross-modulation technique, with pulse modulation of the signal pump beam and 10^{-10} resolution in the frequency shift of probe mode. Results of the experiment agree well with the theoretical analysis based on the mode field configuration. Conditions for realization of QND photon-number measurements determined by thermal nonlinearity are outlined.

1. INTRODUCTION

Recently demonstrated optical whispering gallery mode microresonators, further abbreviated as WGMRs, are characterized by a unique combination of high Q-factor ($Q > 10^8$) and strong mode field concentration (effective volume $V_{\text{eff}} \leq 10^{-8}$ cm^3) [1]. WGMRs are small spheres (typically 40 - 200 μm in diameter) made of fused silica or optical glass, in which light is trapped due to the effect of total internal reflection. The field of high-Q E, H_{lm1} modes is concentrated in a thin near-surface area; external beams are coupled to a resonator by means of prism couplers entering a fringe field of total reflection modes. The maximal obtained quality factor to date is $(1.0 \pm 0.1) \times 10^9$, $\lambda = 633$ nm and $(1.0 \pm 0.3) \times 10^8$, $\lambda = 1150$ nm for fused silica and $(2.0 \pm 0.5) \times 10^7$, $\lambda = 633$ nm for optical glass [2].

Due to their near-micron-size dimensions, WGMRs are characterized by large free spectral range and, therefore, by an extremely high finesse parameter $F = Q/2l$ in excess of 10^6 (l – radial mode index). Easily obtained temperature control of mode frequency allows us to realize, on their basis, miniature tunable narrow-band filters. The temperature tuning 0.7 nm (> 0.1%) with the bandwidth $\Delta\lambda = 6 \times 10^{-5}$ nm for a glass microresonator at $\lambda = 633$ nm was demonstrated [2].

Strong optical fields obtained in these resonators with relatively small pumping power, in combination with high Q-factor, translate into easily observable dispersive optical bistability and mode interaction, even with low-nonlinearity materials such as fused silica. In the case when two modes are taken into consideration, linear dependence of the resonance frequency of one mode on the energy stored in the other mode can be employed for realization of a quantum-nondemolition (QND) photon number measurement experiment [3]. As the first experiments have shown [1], small third-order Kerr nonlinearity ($\chi_K^{(3)} = 1 \times 10^{-14}$ esu) in fused quartz microresonators is added by stronger nonlinear effects identified as thermally induced refraction index changes caused by partial absorption of light in quartz microspheres. It is evident that these effects, which may be also formally described by equivalent third-order susceptibility $\chi_T^{(3)}$, cannot be used for realizing a principally nonabsorptive QND measurement procedure, because the probe mode frequency shift in this case is directly produced by absorbed photons.

In this paper, we report the results of a detailed experimental study of thermal nonlinearity of optical whispering gallery modes in fused silica microresonators. The experiment based on a QND-like two-mode interaction technique included measurement of the nonlinear response of the probe mode resonance frequency on pulse modulation of intensity in the beam coupled to another (signal) mode. The basic result of these measurements was the observation of two types of thermal nonlinearity of WG modes associated with two different heat transport mechanisms and characterized by different response times. The faster mechanism has a typical response time $\tau_{T1} \simeq 5 \times 10^{-6}$ s close to the decay time of oscillations in high-Q modes ($\tau^* \simeq 10^{-7}$ s for $Q = 3 \times 10^8$, $\lambda = 633$ nm). The presence of "fast" thermal nonlinearity imposes strict limitations on the allowed frequency area of the QND photon number measurement.

In real resonators, due to residual nonsphericity and surface inhomogeneity, most of the initially degenerate high-Q whispering gallery modes are split into pairs or larger clusters of closely spaced modes in the frequency domain. In the presence of nonlinearity, this leads to the occurrence of optical multistability. We also observed low-frequency oscillatory instabilities associated with such nonlinear mode clusters.

2. THERMAL NONLINEARITY OF OPTICAL WHISPERING GALLERY MICRORESONATORS

Thermal nonlinearity of optical whispering gallery modes is a particular case of STS-type anharmonicity [4]. This type of optical nonlinearity is observed in media with nonzero optical absorption and results from

the change of the refractive index of the substance under heating produced by partial absorption of light. Since the change in the refractive index is proportional to the intensity of the light beam, the resulting additional polarization is proportional to the third power of the optical field, with the corresponding third-order susceptibility. In the case of plane waves, thermal nonlinearity usually results in self-focusing or self-defocusing effects at high optical powers.

In high-Q dielectric resonators, thermal nonlinearity causes a change in resonant frequencies of modes proportional to their amplitudes squared. In the presence of two (or more) modes with nonzero amplitude, one can distinguish self-action of modes (leading, if large enough, to optical bistability) and their cross-interaction. Since the configuration of the e.m. field of whispering gallery modes is strongly different from that of the plane waves in a continuous medium, the equivalent $\chi_T^{(3)}$ for them must be analyzed on the basis of a heat transport problem for a dielectric sphere with a given localized volumetric heat source. A specific feature of thermal nonlinearity in WGMRs is the presence of two types of thermal relaxation mechanisms. The first, analogous to that of plane waves in continuous media, is thermal relaxation of the e.m. field localization area through heat conductivity with the rest of the dielectric sphere. The second mechanism is connected with thermal relaxation of dielectric sphere as a whole.

Thermal Relaxation of E.M. Field Localization Area with the Rest of the Dielectric Sphere

The e.m. field of high-Q whispering gallery modes E_{lm1}, H_{lm1} is localized in the near-surface area with effective thickness $\delta R \simeq \lambda l^{1/3}/\pi n$ (the estimate is obtained for spherical Bessel functions $j_{l+1/2}(kr)$ and is valid for large indices l; R is the radius of the resonator). The heat conductivity equation in the resonator medium is

$$\dot{T} - D\nabla^2 T = \frac{\omega W}{Q_\alpha c_v}, \qquad (1)$$

where D is the temperature conductivity, $W = n^2E^2/4\pi$ is the density of the e.m. field, $Q_\alpha = 2\pi n/\alpha\lambda$ is defined by absorption α in the resonator material, and c_v is specific heat capacity. From Eq. (1), taking into account the temperature dependence of refractive index $\partial n/\partial T$, one can obtain the equation for additional nonlinear optical susceptibility produced by this thermal effect:

$$\dot{\chi} = -\chi/\tau_T + \chi_T^{(3)}\mathbf{E}^2/\tau_T;$$
$$\tau_{T1} = \frac{(\delta R)^2}{D}; \qquad (2)$$
$$\chi_{T1}^{(3)} = \frac{n(n^2-1)\,\omega\tau_{1T}}{8\pi^2 c_v Q_\alpha}\frac{dn}{dT}.$$

Substituting into expression (2) the parameters of real WGMRs, R = 70 μm ($l = 1 \times 10^3$ at λ = 633 nm), $n = 1.45$, $Q_\alpha = 1 \times 10^9$, $\omega = 3 \times 10^{15}$ s^{-1}, $c_v = 1.5$ erg·K^{-1}, $\partial n/\partial T = 1.3 \times 10^{-5}$ K^{-1}, $D = 8 \times 10^{-3}$ cm^2·s^{-1}, one obtains the following estimates for equivalent third-order susceptibility and the corresponding response time: $\chi_{T1}^{(3)} \simeq 1.5 \times 10^{-13}$ esu, $\tau_{T1} \simeq 3 \times 10^{-6}$ s.

Thermal Relaxation of the Resonator as a Whole

Three main mechanisms contributing to the heat exchange of WGMR with the environment are (1) heat conductivity and convection of the surrounding gas, (2) heat conductivity of support, and (3) thermal radiation. Analysis has shown that if the resonator is not evacuated, the main contribution is determined by convective heat exchange with the surrounding air, because it provides the largest heat flux among the enumerated channels.

The order of magnitude of corresponding $\chi_{T2}^{(3)}$ and τ_{T2} can be evaluated from the equation of convective heat exchange. The result is

$$\tau_{T2} = \frac{R^2}{DNu}, \quad \chi_{T2}^{(3)} = \frac{n(n^2-1)\,\omega\tau_{T2}}{8\pi^2 c_v Q_\alpha}\frac{dn}{dT}\frac{V_{\text{eff}}}{V}, \qquad (3)$$

where V is total volume of the resonator, and Nu is the Nusselt number ($\simeq$0.3 in the air at room temperature). With all of the figures the same as above, we obtain $\chi_{T2}^{(3)} \simeq 5 \times 10^{-12}$ esu, $\tau_{T2} \simeq 1 \times 10^{-2}$ s.

3. DYNAMIC NONLINEAR RESPONSE OF WGMR

In the presence of different nonlinear processes with different relaxation times, the nonlinear response of the resonator becomes dependent on the speed of frequency tuning (if present), as well as on the rate and magnitude of pump intensity modulation. Below, we consider the nonlinear behavior of WGMR in the experimental scheme initially proposed for demonstration of QND energy measurement in a mode. In this scheme, the number of photons N_i stored in one (signal) mode ω_i of resonator is to be monitored via the shift of the resonant frequency of the other (probe) mode ω_k produced by total third-order susceptibility of the resonator material:

$$\omega_k = \omega_{k0}(1 + N_i/N_{ik}^*),$$
$$N_{ik}^* = C_{ik}\frac{n^4 V_{\text{eff}}}{32\pi^2\chi^{(3)}\hbar\omega}.$$

In the initial demonstration scheme, the photon number N_i is modulated by means of intensity modulation of the signal laser beam by rare pulses of variable duration τ_i longer than the decay time of the WG modes $\tau^* \le 1 \times 10^{-7}$ s, the first laser being tuned to the mean frequency of the signal mode. The corresponding readout frequency shift of the probe mode is measured by means of the additional laser tuned to the slope of its nondisturbed resonant curve, or using central tuning and homodyne detection of the probe beam phase. This scheme produces a true QND response on

the pulse modulation of the amplitude in a signal mode only in the case of a fast-response nonlinear mechanism other than absorption. At the same time, it is an instrument for a time-resolved study of different types of third-order nonlinearity mechanisms in optical whispering gallery microresonators.

Let us consider the action of a signal mode amplitude pulse with a duration of τ_i upon the phase of probe wave Φ in the presence of weak "fast" Kerr nonlinearity $\chi_K^{(3)}$ and stronger "slow" thermal nonlinearity $\chi_T^{(3)}$. Let us assume the probe mode amplitude A_p to be much smaller than the amplitude of signal mode A_s, then the initial set of equations takes the form

$$\begin{cases} \dot{A}_p = -A_p/\tau^* - \dfrac{1}{2}P\omega\sin\Phi; \\ \dot{\Phi} = -\dfrac{1}{2}\omega\xi - \dfrac{1}{2}\dfrac{P}{A_p}\omega\cos\Phi \\ \qquad + 2\pi\omega/n^2\,(\chi_K^{(3)}A_s^2 + 2X); \\ \dot{X} = -X/\tau_T + \chi_T^{(3)}\,(A_s^2 + A_p^2)/2\tau_T, \end{cases} \tag{4}$$

where ω is optical frequency, and $\tau^* = 2Q/\omega$ is the decay time of the resonator. Linearization of the system (4) for small deviations from the steady state yields

$$\begin{cases} \dot{a} = -a/\tau^* + \phi A_p^0\cot\Phi^0/\tau^*; \\ \dot{\phi} = -\phi/\tau^* - a\cot\Phi^0/A_p^0\tau^* + 4\pi\omega/n^2\chi \\ \qquad + 2\pi\omega/n^2\chi_K^{(3)}A_s^2; \\ \dot{\chi} = -\chi/\tau_T + a\chi_T^{(3)}A_p^0/\tau_T + \chi_T^{(3)}A_s^2/2\tau_T. \end{cases} \tag{5}$$

Solution of this set of equations under conditions $\tau^* < \tau_i \ll \tau_T$ and $4\pi\chi_T^{(3)}A_p^2\omega\tau^*\cot\Phi^0/n^2 \ll 1$ (the probe mode is in the stable part of the nonlinear resonant curve) yields

$$\phi(t) = \frac{2\pi\omega\tau^*}{n^2}\,[A_s^2(t)\,\chi_K^{(3)} + \frac{\chi_T^{(3)}}{\tau_T}\,(\int A_s^2(t)\,e^{-(t-t_0)/\tau_T}dt - A_s^2(t)\,\tau^*)\,]. \tag{6}$$

It can be seen easily that solution (6) contains two components corresponding to both types of nonlinearity: the instant, directly proportional response of Kerr nonlinearity ($\tau_i > \tau^* > \tau_K$) and the integral term describing the response due to the inertial thermal nonlinearity mechanism. The response caused by the "fast" nonabsorptive nonlinearity will be masked by the thermal one as long as the inequality $\chi_T^{(3)}\tau_i / \chi_K^{(3)}\tau_T > 1$ holds. For short pulses in signal mode ($\tau_i \ll \tau_T$), the second term in Eq. (6) can be written as

$$\frac{2\pi\omega\tau^*\chi_T^{(3)}\tau_i}{n^2\tau_T}A_s^2(t_0)\,e^{-(t-t_0)/\tau_T}. \tag{7}$$

As expected, the thermal response on short pulses is proportional to the duration of pulse τ_i and is accompanied by exponential relaxation with a characteristic time equal to τ_T. It is also evident that in the presence of two types of thermal nonlinearity, solution (6) will be added to by another thermal term with its own $\chi^{(3)}$ and τ.

4. EXPERIMENTAL RESULTS

The schematic diagram of the experimental setup for the investigation of the nonlinear mode interaction in WGMRs is shown in Fig. 1. The optical whispering gallery microresonator, typically 100 - 150 μm in diameter, is placed between two glass prisms with maximal cross dimensions of 0.8 mm. One prism serves to excite the whispering gallery modes, the other one is used as an output coupler for registration of signal and probe mode oscillations. The input prism is immobile, and the resonator and the output prism are independently translated by fused quartz cantilever drives (not shown in Fig. 1). This makes it possible to provide a fine mutual positioning of the resonator and two prisms to obtain the necessary input and output couplings. The whole arrangement is put between two microscope objectives (not shown in Fig. 1) used for focusing signal and probe laser beams from inside the input prism on the touching point with the resonator. The same objectives are used for the formation of narrow output beams which go out from the second prism in the form of comparatively wide nonsymmetric cones. By changing the separation between the resonator and the prisms within the limits $\simeq 0.1 - 1\lambda$, one can adjust the optimal coupling and output loading of WG modes (efficient prism coupling to WG modes in the resonator of given dimensions can be achieved as soon as the unloaded quality-factor Q_0 of WG mode is larger than a certain specific value determined by the maximum prism loading upon touching; for details see Ref. [2]. For typical 100 - 150 μm resonators at $\lambda = 0.63$ μm, ten percent coupling with input beam can be achieved with $Q_0 \geq 10^7$. Signal and probe WG modes are excited in a circular travelling-wave regime in opposite directions so that the corresponding output beams are obtained

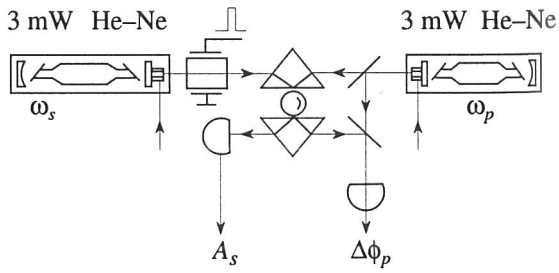

Fig. 1. *A schematic of the experimental setup for investigation of mode interaction in whispering-gallery microresonators.*

from the same sides from which they have been excited. The output signal beam is registered by a photodetector and is used for monitoring the signal mode amplitude. The output beam of the probe mode is then mixed on a beam splitter with the homodyne beam for measuring small deviations of its phase.

Both lasers (signal: 3 mW 35 cm He–Ne and probe: 0.3 mW 12.5 cm He–Ne) are supplied with piezo drives of output mirrors and can be tuned within the limits of laser resonator longitudinal mode separation ($\simeq$ 300 MHz for signal laser and $\simeq$ 1.1 GHz for probe laser) inside the gain curve of the He–Ne mixture. Additional simultaneous tuning possibility ($\simeq$ 10 - 15 GHz) is provided by radiative heating of the resonator (with prisms) with the aid of an incandescent lamp illuminator (not shown).

At the initial stage, both lasers were independently swept by oscilloscope-synchronized sawtooth voltage to detect the resonant WG mode response and adjustment of optimal coupling and resonator temperature. In this regime, we observed typical nonsymmetrical nonreciprocal resonant curves (optical bistability, see Ref. [1]) caused by the self-action of signal and probe modes. The distortion of the resonant curve measured by the length of extended mode response in units of laser frequency sweep depended on the amplitude of excited oscillations and on the rate of the sweep. Typical unloaded Q_0 of WG modes in our experiments with fused silica microresonators was (3 - 6) $\times$ 10^8 (mode bandwidth 0.7 - 1.5 MHz, measured at small coupling), and typical loaded Q_L was (1 - 2) $\times$ 10^8, small-signal bandwidth 2 - 5 MHz. With stronger amplitudes, and more than 5 - 10 μW fed into mode, resonant curves were extended to the Stokes side up to 1 GHz (with 0.3 mW of input power and $\simeq$ 1 GHz·s^{-1} sweep). All the described phenomena were observed easily upon pumping with a stronger signal laser; in this case the discontinuous resonant curves were seen at all sweep rates up to 100 GHz·s^{-1} available with our laser piezodrives. Some of the WG modes displayed the same properties under illumination by a weaker probe laser; in this case subsequent pulse measurements were carried out at reduced probe power (smaller coupling).

At the final stage, the signal laser beam was modulated with the help of an electro-optic shutter by pulses of variable duration 2 $\times$ 10^{-7} - 10^{-4} s. The frequency of the signal laser was pretuned to one of the whispering gallery modes displaying nonlinear response in sweeping regime; precision of tuning was controlled to provide the maximum amplitude of intensity pulses in the output beam of the signal mode. A second laser was adjusted to the frequency of the probe mode by gradually reducing its sweep and controlling the dc voltage on its piezo drive. At this moment, pulsed phase response of the probe wave occurred in the homodyne detector. The small output of the probe mode ($W \simeq$ 0.3 -1 μW) limited the resolution of wide-band (10 MHz) measurements of its frequency shift by the value $\Delta f/f \simeq 1 \times 10^{-10}$ corresponding to phase resolution (0.5 - 1) $\times$ 10^{-1} rad by a homodyne detector, with the loaded quality factor of modes $Q_L \simeq 2 \times 10^8$. A typical response is shown in Fig. 2 ($\tau = 5 \times 10^{-6}$ s, $Q_L = 10^8$). The upper trace is signal mode output; the lower trace is the phase of the probe wave. The exponential relaxation tails of response pulses with characteristic time $\simeq$ 5 μs are easily seen, evidently corresponding to the first type of thermal nonlinearity. The amplitude of this response was approximately proportional to the duration of the pulse inside the interval $\tau_i = 2 \times 10^{-7}$ - 10^{-5} s, in accordance with the results of Sec. 3.

Numerical results of measurements are collected in Fig. 3 in the form of equivalent total $\chi^{(3)}$ evaluated from the amplitude of probe mode response for different signal pulse durations. Also included in Fig. 3 are estimates of $\chi^{(3)}$ for the case of slow variations of signal

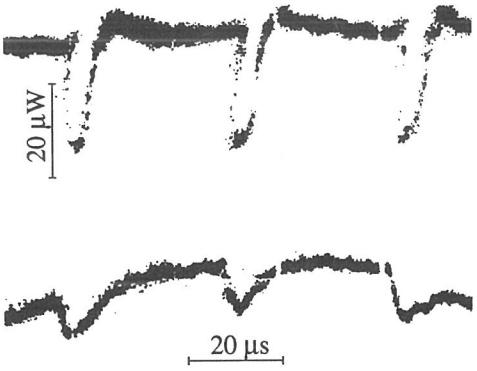

Fig. 2. *Typical thermal-nonlinearity response of probe wave phase on pulsed modulation of signal mode amplitude. Upper trace – intensity of signal wave output beam, lower trace – phase response of the probe mode output beam.*

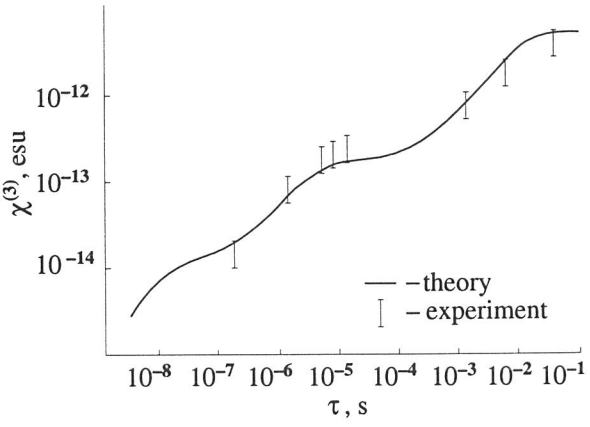

Fig. 3. *Time dispersion of equivalent total $\chi^{(3)}$ for description of cross-modulation of WG modes in a 150 μm fused-silica microresonator, obtained from pulse measurements in mode cross-modulation scheme (τ = 0.2 - 20 μm) and extension of dispersive bistability resonant curves of separate modes in frequency domain (τ = 50 μm - 1 s). Solid line is theoretical prediction taking into account $\chi^{(3)}_{T1}$, $\chi^{(3)}_{T2}$, $\chi^{(3)}_{K}$ and also the reduction of cross-modulation response for pulse durations smaller than $\tau = Q/\omega$, $Q = 3 \times 10^7$, $\omega = 3 \times 10^{15}$ rad·s^{-1} (λ = 633 nm).*

mode amplitudes obtained directly from observations of extended resonant curves during slow frequency sweep. Error boxes of 100% for the value of measured equivalent $\chi^{(3)}$ are due to uncertainty of experimental evaluation of the mode effective volume and absolute amplitudes. In general, the obtained results are in qualitative and quantitative agreement (by the order of magnitude) with the theoretical results of Sec. 2. This concerns both the presence of two types of thermal nonlinearity and predicted values of $\chi^{(3)}_{T1,2}$ and $\tau_{1,2}$. The lowest experimental point obtained for pulse duration $\tau = 0.2$ μs, $\chi^{(3)} = (1.3 \pm 0.5) \times 10^{-14}$ esu corresponds to the nearly pure response of intrinsic fast Kerr nonlinearity of fused silica.

In the course of the experiments, in some resonators possessing pairs of closely spaced modes, we observed optical multistability regimes (Fig. 4) when nonlinear resonant responses of two neighboring modes overlapped. Additionally, in several cases we obtained periodical and quasi-chaotic oscillations in WGMR presumably produced by cyclic transitions of the resonator between two modes (Fig. 5). Similar oscillatory regimes have been observed in single-mode systems in the presence of two nonlinear mechanisms with a different sign of $\chi^{(3)}$ [5]. In our case, however, both Kerr nonlinearity and two types of thermal nonlinearity have the same sign: $\chi^{(3)} > 0$. The observed oscillations can be explained by a slow thermal relaxation mechanism providing conditions for relaxation-type oscillations in the presence of two closely spaced modes. Let the first mode (positioned left along the frequency scan axis in Fig. 4) be excited and the pump frequency be set near the instability point of the nonlinear resonance curve. Suppose that, at a certain moment, the offset of the nonlinear resonance is observed and, within time τ^*, the field amplitude in the resonator drops to nearly zero and the resonator starts cooling down with characteristic time τ_{T2}. Because of the resulting change in n, both modes are shifted to the left, and the second (right) mode becomes tuned to the pump frequency. Due to the buildup of second mode oscillations, the resonator is heated up again and skips to the first mode. The whole cycle is repeated. The period of oscillations due to this mechanism is determined by the slow thermal relaxation time τ_{T2}, absolute value of slow thermal shift of mode frequency Δf_{T2} and by the value of mode splitting δf. In our experiment, the period of oscillations ~ 0.2 ms was in good agreement with the absolute rate of slow thermal relaxation of frequency shift (for the given initial mode amplitude) $\Delta f_{T2} / \tau_{T2} \simeq 20$ MHz·ms^{-1}, and mode splitting $\simeq 5$ MHz.

We should also mention that in many cases, small $\Delta f \leq 10$ MHz splitting of whispering-gallery modes was caused by gradual internal reflection of circular travelling WG resonant waves. This reflection produced small coupling of counter-propagating WG travelling-wave modes and resulted in the occurrence of two resolved resonances corresponding to sine and cosine WG modes. In this case we observed output beams from the second prism coming out in both directions independently of the direction of the exciting beam. Loading of the resonator with a coupling prism led to the widening of both resonance curves and the removal of resolved mode splitting. The backward beam in this case also disappeared. In terms of characteristic times, this means that the lifetime of photons in the resonator became smaller than the beat period of the coupled counter-propagating modes. Naturally, in our pulse modulation two-mode experiments we avoided using such pairs of coupled waves. We used different modes separated usually by 100 - 700 MHz inside an He–Ne mixture gain curve ($\simeq 1.2$ GHz). This led to the necessity of using relatively large 100 - 150 μm WGMRs with closely spaced different modes, although the conditions of small radiation losses (see Ref. [1]) made it possible to reduce the dimensions at least by a factor of 5, with a corresponding reduction of V_{eff} and N^* by a factor of ~ 15 [1]. In our two-mode experiments, a typical V_{eff} was $(1 - 3) \times 10^{-8}$ cm^3 and $N^* = (1 - 3) \times 10^{16}$.

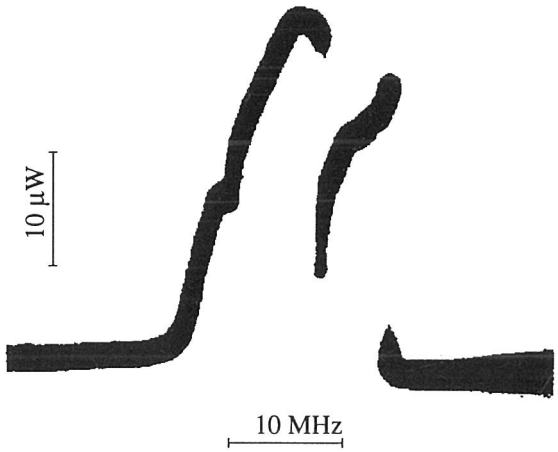

Fig. 4. *Dispersive "reliability" response of a pair of closely spaced WG modes in frequency domain.*

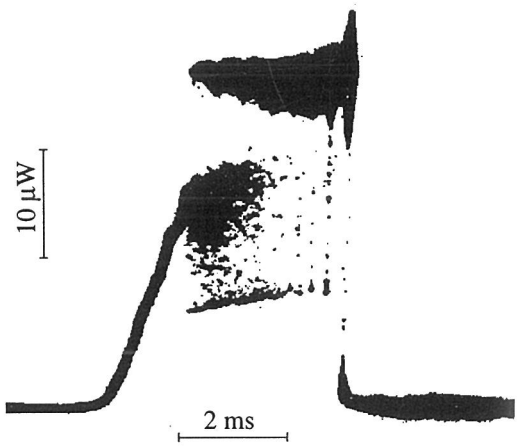

Fig. 5. *Oscillatory instability produced by cyclic transitions between two WG modes.*

5. CONCLUSION

An experimental study of mode interaction in optical whispering gallery microresonators reveals the existence of two types of thermal nonlinearity mechanisms associated with different types of thermal relaxation, in addition to intrinsic Kerr nonlinearity of quartz. One of them is the thermal relaxation of WG mode e.m. field localization area with the rest of the resonator. The other is the thermal relaxation of the resonator as a whole. Experimentally measured values of equivalent thermally-induced third-order susceptibility and relaxation times for the two above mechanisms agree well with the results of the theoretical calculations. With these values of thermal third-order nonlinearities, the contribution of nonabsorptive optical Kerr nonlinearity can be dominant in mode interaction in the case of short pulse modulation of signal mode amplitude $\tau_i < 3 \times 10^{-7}$ s. On the other hand, the amplitude of the signal mode cannot be effectively modulated by pulses shorter than the e.m. decay time of modes $\tau^* \simeq 10^{-8}$ s ($Q = 3 \times 10^7$, $\lambda = 0.63$ μm). Therefore, a demonstration of the QND energy measurement procedure via registration of pulse modulation of signal mode amplitude can be realized in fused silica microresonators only within a small interval of pulse durations. To improve the situation, one can propose (1) to reduce dramatically the loaded Q-factor of modes in order to extend the possible range of QND energy measurements into the area of shorter sample times and higher frequencies at the expense of proportional reduction of sensitivity, and (2) to employ other nonlinear optical materials providing a better proportion of absorptive thermal and nonabsorptive Kerr nonlinearity. For example, optical glasses doped with CdS_xSe_{1-x} microcrystallites possess fast-response third-order nonlinearity on the level up to $\chi^{(3)} \simeq 10^{-9}$ with optical absorption allowing $Q_0 \simeq 10^7$ [6]. Estimates according to Eqs. (2, 3) show that thermal nonlinearity of the optical glass must be smaller, at least by one order of magnitude, than the reported "true" $\chi^{(3)}$ for any sampling time.

ACKNOWLEDGMENTS

The authors would like to thank V.B. Braginskii and S.P. Vyatchanin for helpful discussions. This work was partially supported by the USSR State Committee for Science and Technology.

REFERENCES

1. Braginskii, V.B., Gorodetskii, M.L., and Il'chenko, V.S., 1989, *Phys. Lett. A*, **137**, 393.
2. Vyatchanin, S.P., Gorodetskii, M.L., and Il'chenko, V.S., 1992, *Zh. Prikl. Spektrosk.*, **56**, 274.
3. *Braginskii, V.B. and Il'chenko, V.S.,* 1987, *Dokl. Akad. Nauk SSSR*, **293**, 1358.
4. Klyshko, D.N., 1986, *Physical Foundations of Quantum Electronics* (Moscow: Nauka).
5. Gibbs, H.M., 1981, *Optical Bistability: Controlling Light with Light* (New York: Academic Press).
6. Ainsley, B.J., Girdlestone, H.P, and Cotter, D., 1987, *Electron. Lett.*, **23**, 405.